Calculations of LTE opacities for ICF-target modelling

2006 J. Phys. A: Math. Gen. 39 4781

(http://iopscience.iop.org/0305-4470/39/17/S74)

INSTITUTE OF PHYSICS PUBLISHING JOURNAL OF PHYSICS A: MATHEMATICAL AND GENERAL

J. Phys. A: Math. Gen. **39** (2006) 4781–4786 doi:10.1088/0305-4470/39/17/S74

Calculations of LTE opacities for ICF-target modelling

P A Loboda, D S Netsvetayev, V V Popova and L B Samolovskikh

Russian Federal Nuclear Center—All-Russian Institute of Technical Physics (RFNC VNIITF), POB 245, Snezhinsk, Chelyabinsk region, 456770, Russia

E-mail: p.a.loboda@vniitf.ru

Received 16 October 2005, in final form 17 January 2006
Published 7 April 2006
Online at stacks.iop.org/JPhysA/39/4781

Abstract

Using the SPECTR numerical model based on the (super)configuration approach, Rosseland mean opacities of the Cu-doped Be plasmas were calculated in broad temperature and density ranges in application to the modelling of promising indirect-driven targets proposed for future ICF experiments. Comparisons of mid-ionized plasma opacities to experimental and other theoretical data are also presented.

PACS numbers: 52.25.Jm, 52.25.Os

1. Introduction

Modelling of radiative hydrodynamics for the problems of the inertial confinement fusion (ICF) research and other fields of high energy density physics calls for reliable data on spectral and mean opacities of various hot, dense plasmas. These data, in turn, imply a realistic description of plasma photoabsorption spectra in broad temperature and density ranges. A major challenge here is presented by the line-absorption constituent whose contribution to radiative losses and opacity frequently appears to be essentially important. Specifically, for mid-ionized dense plasma of mid- and high-Z elements, the number of well-populated states of multielectron ions with open shells may be extremely large, especially at local thermodynamic equilibrium (LTE), thus giving rise to a huge number of radiative transitions in various ions responsible for manifolds of unresolved overlapping lines covering broad spectral regions.

A series of recent special-purpose experimental studies of radiative properties of hot, dense matter (see, for example, [1–8]) shows that the most adequate interpretation of such spectra is now reached on the basis of the (super)configuration approach. That approach uses an averaged description of spectra associated with j–j ('relativistic') one-electron transitions between configurations of plasma ions or groups of energetically adjacent configurations—so-called superconfigurations [9]. In the cases allowing detailed configuration accounting (DCA), this description generally uses the models considering unresolved j–j transition arrays between

(relativistic) sub-configurations (relativistic UTAs, or SOSAs—spin-orbit-split arrays) [10] or nonrelativistic configurations (j-transition arrays—JTA) [11].

In a more general situation, when the number of essentially populated configurations of plasma ions may be enormous, a tractable modelling of unresolved spectral structures is obtainable within the framework of the superconfiguration (SC) approach on the basis of the STA (super transition arrays) model, first formulated by Bar-Shalom and co-workers [9]. In that model, the entire spectral structure attributed to a specific one-electron j–j transition is represented by a small number of the STAs comprising all possible UTAs (JTAs) for the same transition between pairs of superconfigurations.

Ionization balance and populations of (super)configuration states are governed by the Saha–Boltzmann equation allowing for electron-degeneracy and plasma-nonideality effects. The configuration populations within superconfigurations are assumed to obey the Boltzmann distribution, as directly supported by the LTE conditions. In line with the DCA models, the SC approach also makes an essential approximation that the plasma temperature is high enough to adopt a statistical distribution of the energy-level populations of any specific configuration. It is worth noting that similar assumptions for the SC population statistics, utilizing an effective excitation temperature within each superconfiguration, have been successfully employed in the SC collisional radiative models to describe radiative properties of hot, dense plasmas under non-LTE conditions [12–16].

Following the (super)configuration approach, we have developed the SPECTR numerical model for simulating photoabsorption spectra of LTE plasmas of various elements and mixtures and calculated the opacities of the Cu-doped Be plasmas in application to the modelling of indirect-driven laser fusion targets.

2. The SPECTR model

At present, the SPECTR model implements a simplified variant of the STA model [9, 17] stemming from direct generalization of a more detailed JTA description accounting for configuration-interaction effects [11]. Specifically, superconfiguration energies and partition functions as well as the moments of STAs are found on an optimized temperature grid using average energies, statistical weights, and the moments of the constituent nonrelativistic configurations and JTAs. In addition, supershells, comprising superconfigurations $\left\{\Xi_k^Q\right\}$ of a Q-electron ion of an element k, are assumed to collect all the nl-shells with the same principal quantum number n and, therefore, coincide with atomic shells: $\Xi_k^Q = \mathrm{K}^{q_1}\mathrm{L}^{q_2}\mathrm{M}^{q_3}\mathrm{N}^{q_4}\cdots, \sum_i q_i = Q$.

All the configuration and configuration-transition quantities are pre-calculated from single- and two-electron orbital data generated with the modified RCN36 and RCN2 modules of the well-known Cowan atomic structure code [18] based on the Hartree–Fock method with relativistic corrections (HFR-method). Spectral distributions of STAs are represented by the Voigt profile, being the convolution of the Gaussian and Lorentzian profiles. The Gaussian contribution is responsible for statistical broadening (JTA variances and variance of JTA average energies in STAs) and Doppler broadening, while the Lorentzian one is for radiative and collisional broadening of spectral lines belonging to a given STA. Ionization balance is found from the Saha–Boltzmann equation allowing for electron-degeneracy and plasma-nonideality effects. The latter are described by using the ion-sphere prescription (see for example [19]) through the ionization potential lowering and truncation of partition functions. Total energy-dependent opacity $\kappa(\varepsilon)$ is given by the sum of photoabsorption coefficients due to bound–bound transitions in STAs, bound–free photoionization transitions, free–free inverse-bremsstrahlung transitions and Compton scattering. Free–free and bound–free absorption

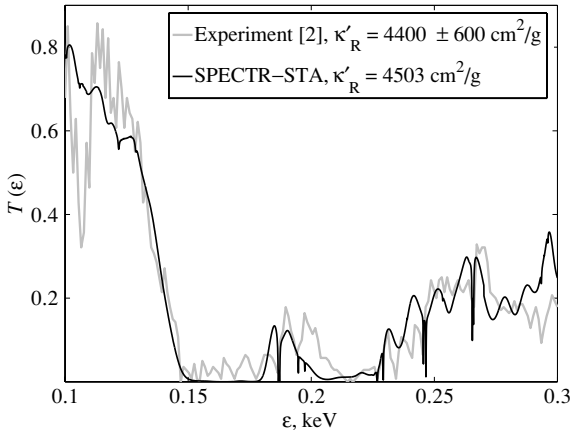

Figure 1. LTE-transmission spectra of the Fe-component in a 300 μm long sample of Fe:NaF plasma at a temperature $T = 59$ eV and total density of $\rho = 0.0113$ g cm^{-3}, by 80.2% weight iron, compared to experimental transmission data of [2].

are treated in the Born–Elwert [20] and Kramers approximations, respectively, and Compton scattering is calculated using analytic interpolation [20] based on the Klein–Nishina formula.

To test the created numerical model, the transmission spectrum of iron in the LTE Fe:NaF plasma was calculated with the follow-on comparison of the Rosseland mean opacity (see, for example, [21]),

$$\frac{1}{\kappa_R} = \frac{15}{4\pi^4}\int_0^\infty \frac{1}{\kappa(\varepsilon)}\frac{u^4\,\mathrm{e}^{-u}}{(1-\mathrm{e}^{-u})^2}\,\mathrm{d}u, \qquad u = \frac{\varepsilon}{T}$$

(the temperature T is in energy units), referred to a specified spectral region—κ'_{R}, to the data of a special-purpose benchmark experiment and previous calculations done with more elaborate theories [1, 2].

Figure 1 presents the comparison of the SPECTR–STA-calculated and measured transmission spectra $T(\varepsilon) = \exp[-\kappa(\varepsilon)\rho L]$ of iron in an $L = 300$ μm long sample of Fe:NaF plasma, with a composition of 80.2% wt iron, at a temperature $T = 59$ eV and total mass density $\rho = 0.0113$ g cm^{-3}. Under these conditions, the opacity of iron plasma is governed by the bound–bound and bound–free photoabsorption by the ions with the open L- and M-shells. It is seen from the figure that the model provides rather good agreement of the calculated $T(\varepsilon)$ spectrum with the experimental data. Furthermore, the Rosseland group mean opacity (over the spectral region $\varepsilon = 100$–300 eV) obtained with SPECTR–STA, $\kappa'_{\mathrm{R}} = 4503$ cm^2 g^{-1}, agrees closely both with the experimental value of 4400 ± 600 cm^2 g^{-1}, and the results given by the STA [9] and MCUTA (UTA with Monte Carlo-sampled configurations) models: 4630 and 4525 cm^2 g^{-1}, respectively [1, 2].

3. Opacities of the Cu-doped Be plasmas

The SPECTR–STA model was employed to calculate plasma opacities of Cu-doped Be (at a level of 1–2% atomic fraction of Cu) being evaluated as a promising material for radiation-driven imploding shells (ablators) of ICF capsules [22–25] for future experiments on the megajoule-class laser facilities NIF (National Ignition Facility) [26] and Iskra-6 [27]. Here,

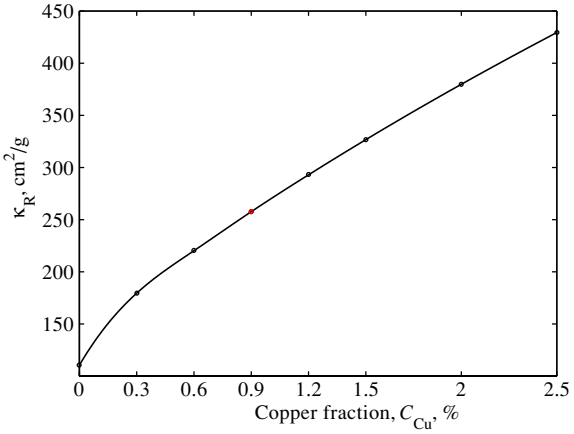

Figure 2. Dependence of Rosseland mean opacity of the Be:Cu plasma at $\rho = 0.1$ g cm^{-3} and $T = 100$ eV on the Cu atomic fraction.

the copper dopant is employed to provide the requisite value of Rosseland mean opacity $\kappa_R^{Be:Cu}$ of the ablator for optimal radiation drive.

Calculations of compression and burn of a promising candidate of the relevant capsule for achieving ignition on NIF [22–24] showed that the highest energy yield is gained at a copper atomic fraction of 0.9%. In similar calculations [25] for a smaller-scale target done by our colleagues for the conditions anticipated in future experiments on the Iskra-6 facility, the optimal copper atomic fraction appeared to be approximately twice as much (2%) when employing the data on Rosseland means obtained by using an average-atom model. However, those data were later found to be less accurate than the SPECTR–STA predictions due to insufficient description of the L- and M-shell line-absorption contributions.

Therefore, using the SPECTR–STA model we examined the dependence of Rosseland mean opacity of the Be:Cu plasma on the Cu atomic fraction C_{Cu}, $\kappa_R^{Be:Cu}(C_{Cu})$, at typical densities and temperatures of the ablator, $\rho = 0.1$ g cm^{-3}, $T = 100$ eV [25] (see figure 2), and calculated the values of $\kappa_R^{Be:Cu}(\rho, T)$ at several C_{Cu} in a broad range of temperatures and densities, $T = 10$–360 eV, $\rho = 10^{-3}$–10 g cm^{-3} [25], anticipated in future ICF experiments on the NIF and Iskra-6 facilities.

The calculated data show that plasma opacity for the conditions of interest may vary over more than 3 orders of magnitude. This is exemplified in figure 3 presenting the Rosseland means of the Be(99.1%):Cu(0.9%) plasma. One can also see from figure 2 that at typical temperatures and densities of the ablator, admixtures of 0.9 and 2 at.% copper are responsible for about 60 and 70% of the respective total Rosseland mean opacities, increasing, in turn, to 2.3 and 3.5 times relative to pure Be, respectively.

Such a drastic increase in opacity occurs due to the line absorption of multielectron copper ions, mostly due to the L-shell absorption at relatively high photon energies ($\varepsilon \gtrsim 0.9$ keV), to which Be is transparent, thus enabling one to get the balanced spectral absorption necessary for achieving optimal compression performance of the ICF capsule. This fact is illustrated in figure 4 with spectral opacities of pure Be and the Be(99.1%):Cu(0.9%) plasmas at $\rho = 0.1$ g cm^{-3} and $T = 100$ eV. Thus, the calculated Rosseland mean opacities $\kappa_R^{Be:Cu}(\rho, T, C_{Cu})$ may be employed for the refinement of previous ICF-capsule modelling [25] and further optimization of the ICF target designs with radiation-driven Be:Cu-ablators.

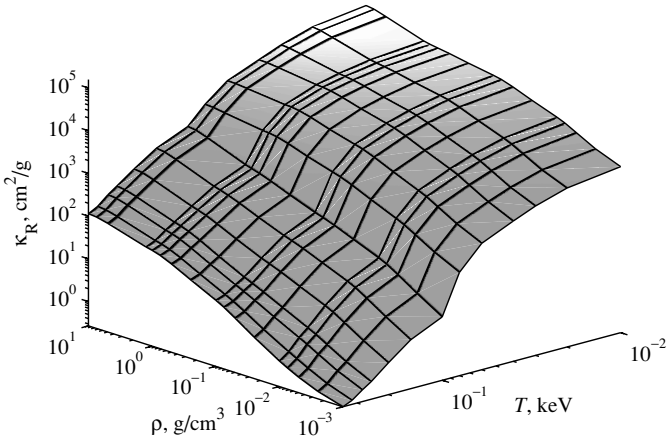

Figure 3. Rosseland means of the Be(99.1%):Cu(0.9%) plasma as calculated with SPECTR–STA.

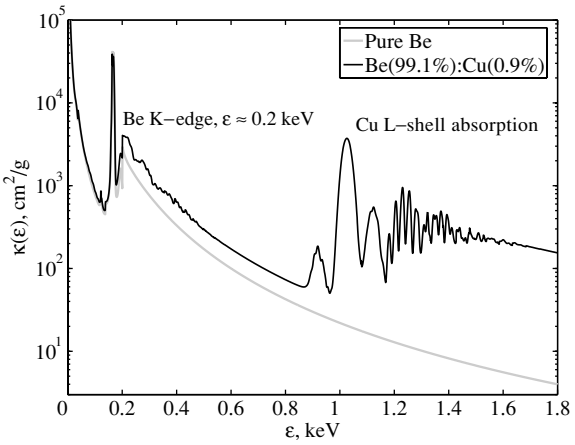

Figure 4. Spectral opacities of pure Be and the Be(99.1%):Cu(0.9%) plasmas at $\rho = 0.1$ g cm^{-3} and $T = 100$ eV.

4. Conclusion

To calculate spectral and energy-averaged mean opacities of hot, dense LTE plasmas of various elements and mixtures we have developed the SPECTR numerical model implementing a simplified variant of the STA model [9, 17]. Comparisons of spectral and Rosseland mean opacities of mid-ionized Fe:NaF mixture revealed pretty good agreement of the SPECTR–STA results with experimental and other theoretical data [1, 2].

With SPECTR–STA, Rosseland opacities of the Cu-doped Be were calculated in broad temperature and density ranges in application to the hydromodelling of promising ICF capsules with the Be:Cu ablators [25]. The contribution due to line absorption of copper ions, mostly represented by the L-shell absorption, was found to dominate total Rosseland opacities of the Be:Cu plasma at typical temperatures and densities of the ablator, being strongly dependent on the Cu-admixture fraction.

At present, the SPECTR–STA model is being extended and improved to implement the most powerful features of the original STA model [9, 17] that would enable one to account for all possible configurations within the constraints of high-Z elements with open M-, N-, O-shells and therefore to appropriately describe the opacities of the mixtures of those elements.

References

[1] Springer P T *et al* 1992 *Phys. Rev. Lett.* **69** 3735–8
[2] Springer P T *et al* 1994 *J. Quant. Spectrosc. Radiat. Transfer* **51** 371–7
[3] Springer P T *et al* 1997 *J. Quant. Spectrosc. Radiat. Transfer* **58** 927–35
[4] Goldstein W H *et al* 1993 *Phys. Rev.* E **47** 4349–53
[5] Young B K F, Wilson B G, Price D F and Stewart R E 1998 *Phys. Rev.* E **58** 4929–36
[6] Foord M E *et al* 2000 *Phys. Rev. Lett.* **85** 992–5
[7] Glenzer S H, Fournier K B, Wilson B G, Lee R W and Suter L J 2001 *Phys. Rev. Lett.* **87** 045002
[8] Bauche J *et al* 2003 *J. Quant. Spectrosc. Radiat. Transfer* **81** 47–55
[9] Bar-Shalom A, Oreg J, Goldstein W H, Shvarts D and Zigler A 1989 *Phys. Rev.* A **40** 3183–93
[10] Bauche-Arnoult C, Bauche J and Klapich M 1985 *Phys. Rev.* A **31** 2248–59
[11] Bar-Shalom A, Oreg J and Goldstein W H 1994 *J. Quant. Spectrosc. Radiat. Transfer* **51** 27–39
[12] Bar-Shalom A, Oreg J and Klapich M 1997 *J. Quant. Spectrosc. Radiat. Transfer* **58** 427–39
[13] Bar-Shalom A, Oreg J and Klapich M 2000 *J. Quant. Spectrosc. Radiat. Transfer* **65** 43–55
[14] Peyrusse O 2000 *J. Phys. B: At. Mol. Opt. Phys.* **33** 4303–21
[15] Busquet M, Klapich M and Bar-Shalom A 2001 *J. Quant. Spectrosc. Radiat. Transfer* **71** 225–36
[16] Bauche J, Bauche-Arnoult C and Fournier K B 2004 *Phys. Rev.* E **69** 026403
[17] Bar-Shalom A, Oreg J and Goldstein W H 1995 *Phys. Rev.* E **51** 4882–90
[18] Cowan R D 1981 *The Theory of Atomic Structure and Spectra* (Berkeley, CA: University of California Press)
[19] More R M 1989 *Physics of Highly-Ionized Atoms* ed R Marrus (New York: Plenum) pp 419–69
[20] Nikiforov A F, Novikov V G and Uvarov V B 2000 *Quantum-Statistical Models of Hot Dense Matter and Methods for Computation Opacity and Equation of State* (Moscow: Fizmatlit)
[21] Zel'dovich Ya B and Raizer Yu P 1967 *Physics of Shock Waves and High-Temperature Hydrodynamic Phenomena* (New York: Academic)
[22] Krauser W J *et al* 1996 *Phys. Plasmas* **3** 2084–8
[23] Wilson D C *et al* 1998 *Phys. Plasmas* **5** 1953–9
[24] Dittrich T R *et al* 1999 *Phys. Plasmas* **6** 2164–70
[25] Karlykhanov N G, Lykov V A, Timakova M S and Chizhkov M N 2004 *JETP Lett.* **79** 25–7
[26] Campbell E M and Hogan J W 2000 *Inertial Fusion Sciences and Applications—99* ed C Labaune *et al* (Oxford: Elsevier) p 9
[27] Kirillov G A *et al* 2000 *Laser Part. Beams* **18** 219